metals

MDPI

Article

Large-Scale Atomistic Simulation of Sintering Process and Mechanical Properties of Al Matrix Composite with Different Reinforcements

Yongchao Zhu [1,*], Can Sui [1], Na Li [2], Lijuan Sun [1] and Songtao Li [1,*]

[1] Department of Railway Engineering, Zhengzhou Railway Vocational and Technical College, Zhengzhou 451460, China; suican@zzrvtc.edu.cn (C.S.); sunlijuan@zzrvtc.edu.cn (L.S.)
[2] School of Mechanics and Engineering Science, Zhengzhou University, Zhengzhou 450001, China; zzulina@zzu.edu.cn
* Correspondence: zhuyongchao@zzrvtc.edu.cn (Y.Z.); lisongtao@zzrvtc.edu.cn (S.L.)

Abstract: Through molecular dynamics methods, composite models built with a large scale were employed to investigate the effects of different reinforcements, which were different from those used in most of the similar studies, where only a graphene nanosheet (GNS) or a rigid spherical particle was embedded in a metal matrix. Here, 27 GNSs or diamond particles were placed in the empty spaces between Al particles with random directions. Then, Al matrix composites were prepared by modeling a sintering process. Structural analysis and tensile modeling were carried out on the sintered composites. The results indicate that the density of the Al–graphene composite was higher and increased with growth in the size of the reinforcements, although the Al–graphene system required more heating time to achieve densification. Bigger GNSs were likely to increase the pore volume of the composite. Meanwhile, larger GNSs were also more beneficial for grain refinement, leading to growth in the ratio of Al atoms at grain boundaries. The greater impact of GNSs on the inner structure was not just derived from their high specific surface area, and this impact was enlarged if drawn as a function of the weight fraction rather than the surface area. However, tensile processes revealed that two-dimensional (2D) materials seemed to have no clear impact on the direct strengthening effect, and anisotropy could not be observed in the large-scale models. The biggest GNSs even led to reductions in both the tensile strength and ductility of the Al–graphene composite, which coincided with some experimental reports. The evolution of the inner structures indicated that GNSs have the same role as diamond particles in dislocation accumulation and crack propagation. The major advantage of GNSs is their ability to improve the densification and grain refinement of the metal matrix composite (MMC).

Keywords: molecular dynamics; graphene; diamond; composite; mechanical property

Citation: Zhu, Y.; Sui, C.; Li, N.; Sun, L.; Li, S. Large-Scale Atomistic Simulation of Sintering Process and Mechanical Properties of Al Matrix Composite with Different Reinforcements. *Metals* **2024**, *14*, 1312. https://doi.org/10.3390/met14111312

Academic Editor: Abdollah Saboori

Received: 22 September 2024
Revised: 14 November 2024
Accepted: 19 November 2024
Published: 20 November 2024

1. Introduction

Recently, many efforts have been made to study the effects of two-dimensional (2D) reinforcement on metal matrix composites. Compared with three-dimensional (3D) reinforcement, graphene is regarded as a more hopeful reinforcement for metal matrix composites (MMCs), as it leads to comprehensive improvements in wear, strength, and stability [1]. However, most studies only reported the beneficial effects of graphene nanosheets (GNSs) on MMCs, and the improvements were simply ascribed to the high specific surface area or the excellent mechanical properties of graphene [2,3]. The underlying mechanism is still unclear, and some conclusions are not very scientific, as they are based on inappropriate comparisons between different reinforcements.

In most simulations, GNSs proved to be a more effective reinforcement for MMCs, based on a simple model where only a graphene nanosheet was embedded in a metal

matrix. Anisotropy in the mechanical properties could be observed, as well as apparent improvements in strength and ductility. Zhao et al. reported a folded graphene-reinforced copper nanocomposite that exhibited simultaneous enhancements of 2.26% in strength and 32.38% in ductility [4]. Liu et al. built a model of a graphene-reinforced Al composite with a modified substrate surface, showing amazing improvements of 198.15% in ultimate strength and 185.71% in ultimate strain [5]. Zhu et al. established models of wrinkled graphene/aluminum, attributing the overall enhancement to the synergistic influence of the geometric structure, grain refinement, dislocation blocking, grain boundary strengthening, and nanotwin strengthening [6]. Srivastava et al. compared the effects of GNSs on the compressive strengthening behavior of a composite in the zigzag and armchair directions, which increased by 210% and 240% compared to pure Al [7]. In these models, the mechanical properties of metal–GNS composites were compared with a pure metal model rather than composites reinforced by 3D particles. Nevertheless, all these studies employed simple models by introducing a GNS as large as the metal matrix. Undoubtedly, the load was applied on the graphene directly, giving rise to an overall enhancement of the MMC.

Furthermore, most experimental research has focused on the effects of the graphene content on mechanical properties, taking graphene as a continuous rectangular platelet to develop theoretical models. Elkady et al. added 0.2 wt.% of GNSs to an Al/Ni alloy via the hot pressing technique, obtaining increases of 30.22% in compressive strength and 43.75% in strain [8]. Lou et al. introduced 0.5 wt.% of GNSs to an Al matrix by hot extrusion, improving the tensile strength from 71.77 MPa to 164.49 MPa and improving the elongation from 0.76% to 21.81% [9]. Zeng et al. prepared 3D graphene network-reinforced Al matrix composites by powder metallurgy. They exhibited the same favorable toughness as pure aluminum with an improvement in ductility [10]. Zhou et al. fabricated GNS/Ni composites by two-step 3D vibration milling, generating an increase of 33.94 in tensile strength and a reduction of 11.56% in elongation [11]. Yang et al. sintered Al–graphene composites by the pressure infiltration method, showing an increase of 45% in tensile strength and a decrease of 44% in elongation after the addition of 0.54 wt.% GNSs [12]. Wang et al. explored a maximum increase of 30.6% in the tensile strength of Al–graphene composites, but the elongation dropped from 60% to 24% when the graphene content exceeded 0.5 wt.% [13]. Although the additions of GNSs in these studies were generally less than 1 wt.%, the improvements were even higher compared with composites enhanced by 3D reinforcement contents of more than 10 wt.% [14–16]. However, it is not difficult to find that there are wide gaps in strength between the experimental results, let alone the fundamental differences in ductility between experiments and models. Limited by experimental methods, the effects of reinforcement on the evolution of inner structures cannot be studied as effectively.

Since the simulated results cannot be completely supported by experimental reports and the structures of simple models in simulations are vastly different from experimental samples, a large-scale model was designed here to discuss the effects of different reinforcements on MMCs in detail. The designed models comprised dozens of reinforced GNSs or diamond particles that were placed in random locations. The sizes of the different reinforcements were also designed to obtain results as functions of surface area and weight fraction. Thus, the effect on an MMC could be studied more accurately, avoiding systematic errors such as the directional distribution of GNSs and direct loading on graphene.

2. Model Methods

To produce a large-scale model of an Al matrix composite for this molecular dynamics (MD) simulation, the basic structure of an Al reinforcement system was built, which consisted of 27 spherical Al particles and 27 reinforced nanosheets or nanoparticles. As shown in Figure 1, graphene was chosen to serve as a 2D reinforced phase, while diamond was selected to act as a 3D reinforced phase. To insert these reinforcements into the spaces between the Al particles, adjacent Al particles were set to be 2 Å apart from each other. In

all models, the Al spherical particles had the same radius of 24 Å. However, the sizes of the graphene nanosheets and diamond particles were different, as listed in Table 1. Thus, the effects of the two kinds of reinforcements with respect to the same surface area or weight content could be studied. Because the simple models in most MD simulations contain only a piece of a GNS, the composite models exhibited obvious anisotropy in their mechanical properties. Nevertheless, anisotropy has not been reported in experimental studies because experimental samples contain large quantities of GNSs that are dispersed randomly by ball milling or stirring. Therefore, the orientation of every nanoparticle was random here to avoid a directional distribution of reinforcements, especially in the Al–graphene system. Besides the composite models, a model comprising only 27 Al particles was used as a baseline for comparisons between composite models with different reinforcements. In order to use every model as a representative volume element (RVE) in an Al matrix composite, periodic boundary conditions (PBCs) were applied in the three dimensions of the simulation box.

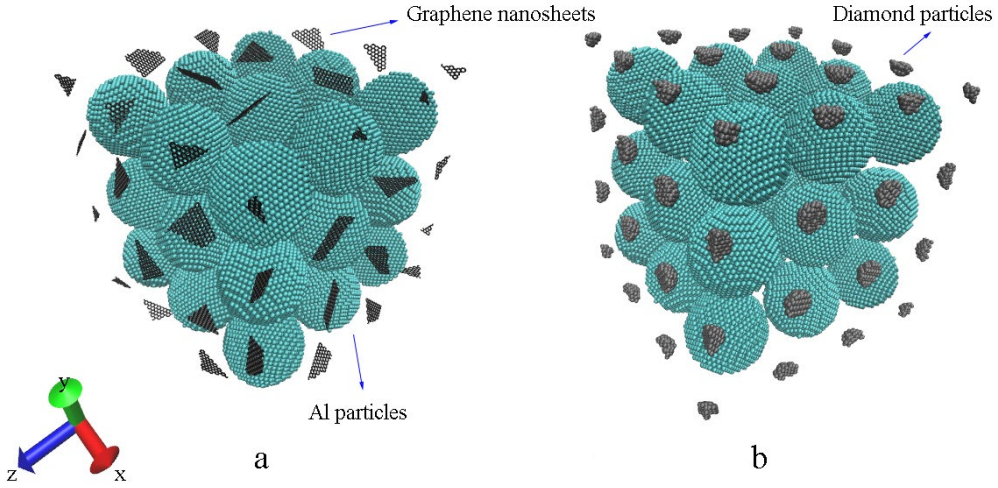

Figure 1. Models of composite systems before sintering. (**a**) Al–graphene system. (**b**) Al–diamond system.

Table 1. The sizes of the different reinforcements.

Side Length (l_s) (Å)	Graphene Surface Area (Å^2)	Weight Content (%)	Radius (R) (Å)	Diamond Surface Area (Å^2)	Weight Content (%)
3.5	194.6	0.6	4.0	199.6	0.8
7.0	778.5	4.8	8.0	798.2	4.0
10.5	1751.7	15.8	12.0	1796.0	7.0

Before sintering, every model was relaxed for 100 ps in an NPT ensemble at 300 K and 1 atm because the particles were not close to each other in the initial model. Then, all composite systems with gathered nanoparticles went through the same process of heating, holding, and cooling, and every process lasted 300 ps. This meant that every model was heated from 300 K to 773 K and then dropped back to 300 K. Meanwhile, the pressure of every model was increased from 1 atm to 500 atm and then reduced to 1 atm. The settings above were fixed on the basis of similar studies that modeled the sintering process of an Al matrix composite [17,18].

After sintering, a tensile process was conducted on the sintered system. By changing the shape of the simulation box in a direction, quasi-static tension operated under the NVE ensemble at 300 K, with the temperature reset by explicitly rescaling the velocities. The tensile properties of every sintered system were measured separately in three orthogonal directions.

To compare the results with studies based on a simple model of an Al matrix composite, the Al–Al, C–C, and Al–C interactions took the style of *eam*, *tersoff*, and *morse* potentials, respectively, which were the settings used in [19,20]. At the runtimes of the MD models, the velocity *Verlet* algorithm was applied, and the time step was set to 1.0 femtosecond. Here, LAMMPS (3 Mar 2020) software was used to operate all the MD simulations, and VMD (1.9.3) software was employed to visualize the results of the simulations.

3. Results and Discussion

3.1. The Sintering Process

Because there was a clear gap in volume between the 2D and 3D reinforcements, the total volumes of the Al atoms were monitored to study the sintering process. At the beginning, the difference in the volumes of the Al atoms was very large, as shown in Figure 2 from 0 ps to 100 ps, because empty spaces existed between the particles in the initial models, and different parts of the empty spaces were regarded as the Voronoi volumes of the Al atoms based on the sizes and locations of the reinforcements. After 100 ps of relaxing time, the composites started to become compacted. As the graphene was easy to bend, it was very likely to form an enclosed space, which was counted as a part of the Voronoi volume of the Al atoms in the Al–graphene system. In the enlarged area in Figure 2, it can be seen that the larger the size of the graphene, the more space the Al atoms in the composite occupied at the beginning of the sintering process (100 ps). While heating up, the Al volumes in all models dropped quickly. However, the Al volumes in the Al–diamond reached the lowest point faster, while the Al volume in the composite with the largest GNSs did not reach the lowest point until the heating stage had almost ended. Then, thermal expansion brought an increase in the volume. From this moment on, primarily, densification of Al atoms was accomplished. Then, a slight decrease appeared in the stable environment, followed by a cold shrink. Overall, the Al volume in the pure Al model was the largest, while the Al volumes in the composites decreased with increases in the sizes of the reinforcements in both the Al–diamond and Al–graphene. Moreover, the Al volume in the Al–diamond was bigger than that in the Al–graphene, and this became more noticeable as the sizes of the reinforcements got bigger. In consideration of the bigger volume of the Al atoms in the Al–graphene at the start, it was not difficult to conclude that graphene is more conducive to promoting densification of a metal matrix composite.

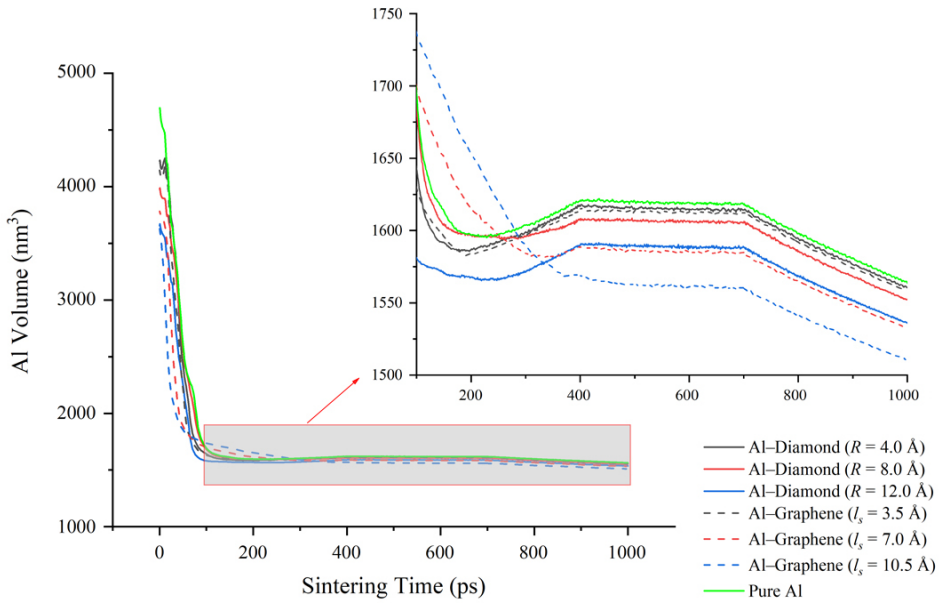

Figure 2. The volumes of the composites as a function of the sintering time.

3.2. The Sintered Structure

Structural analysis was carried out on the sintered composites to identify their densities, interfacial atoms, and pore volumes. The sizes of the different reinforcements are listed in Table 1, and there was a very small difference in the surface areas between the GNSs and the diamond particles. Therefore, the effects of the different reinforcements could be compared using the same surface area. According to Figure 3a, the density values of the Al matrix composite were very close to experiment reports [15]. However, the MD models here revealed that the Al matrix as well as the total structure of the Al–graphene had higher densities. Both the total and Al densities of the Al–graphene with the smallest GNSs were a little higher than those of the Al–diamond, and the gap was no more than 0.03 g/cc even if the sizes of the reinforcements became larger. If the density curves were drawn as functions of the weight fraction as in most experimental studies, graphene had a greater advantage of more than 0.05 g/cc for densification. Therefore, it was concluded that graphene is more helpful for improving composite density, mainly because it promotes densification of the metal matrix.

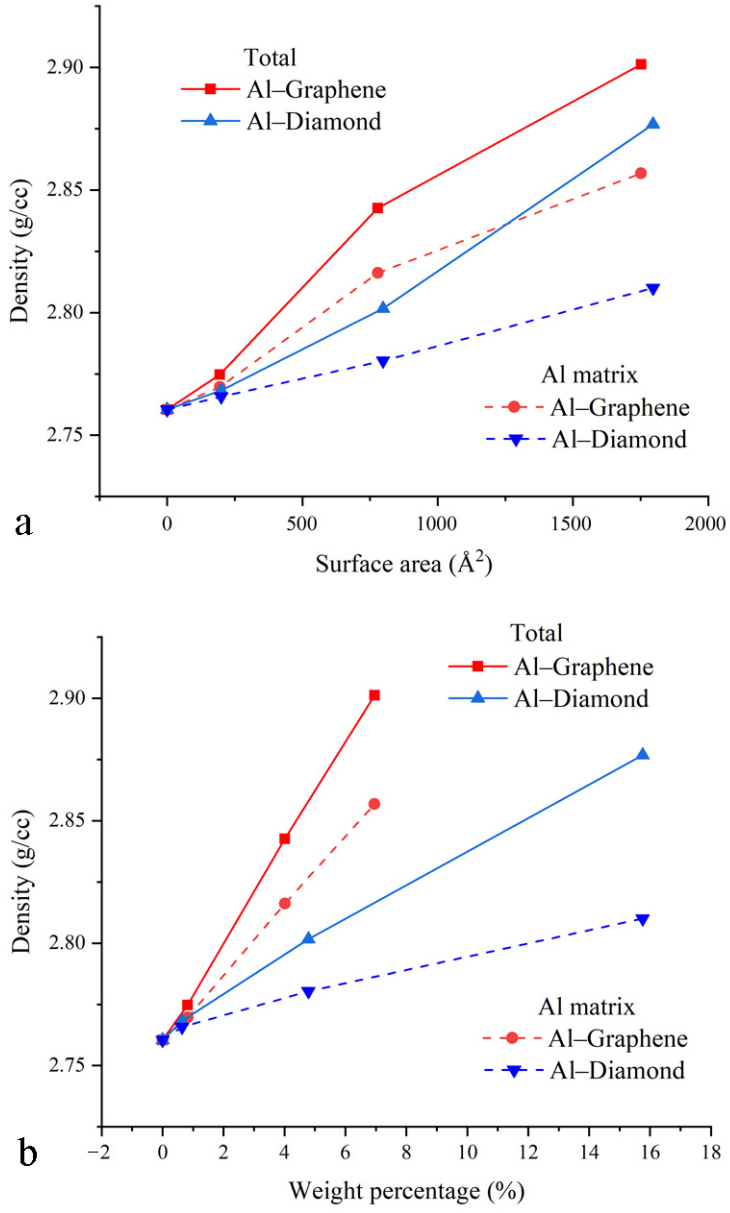

Figure 3. The densities of the composites as functions of the surface area (**a**) and weight fraction (**b**).

To gain insight into the inner structures of the composites, the Al atoms were colored based on their values for the centro-symmetry parameter (CSP). The arrangements of the Al atoms around the reinforcements in Figure 4 are visibly disturbed. When the sizes of the reinforcements were small, the GNSs and diamond particles seemed to have no effect on the local structure. As the reinforcements grew in size, the GNSs exerted more influence on the structure of the Al matrix than the diamond particles. The full blue areas representing perfect lattices were fewer and smaller in the Al–graphene, and more grain boundaries could be found along the GNSs. This grain refinement was quantified by common neighbor analysis (CNA), as shown in Figure 5. Compared to the model without reinforcement, the GNSs and diamond particles increased the ratio of Al atoms at the grain boundaries from 41.4% to 76.4% (Al–GNS) and 61.6% (Al–diamond). As shown in a structure with an l_s of 10.5 Å, it was difficult to identify an area of perfect lattice when the l_s of the GNSs was 10.5 Å. Therefore, it was confirmed that graphene is more helpful for grain refinement in a metal matrix.

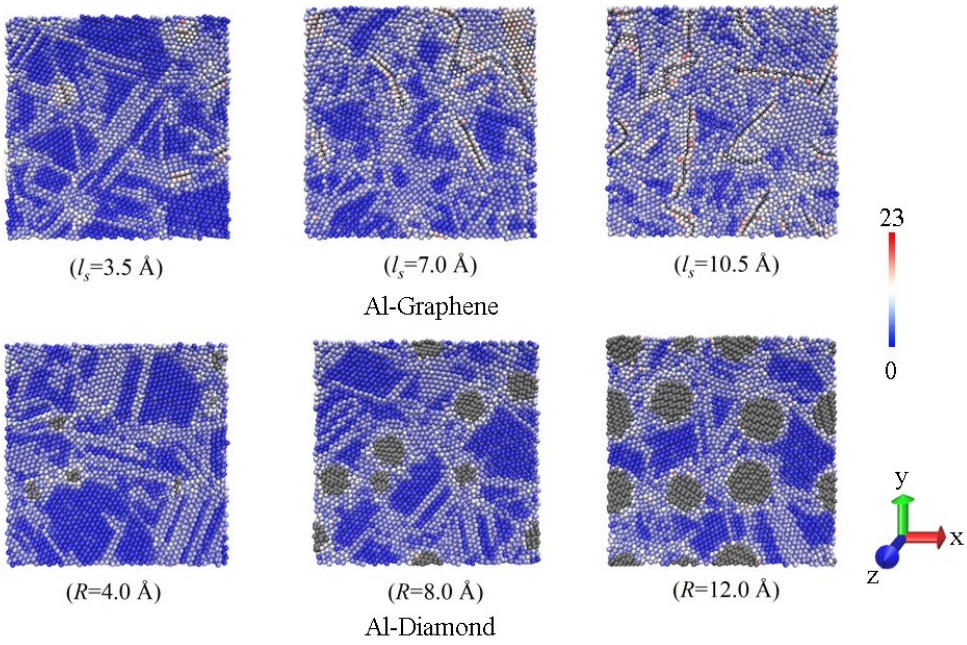

Figure 4. Inner structures of composites, where Al atoms are colored based on CSP values and reinforcements are tinted black.

The volumes of nanopores were also calculated to characterize the inner structure. An increase in the size of the reinforcements also gave rise to nanopore growth from 135 Å^3 to 449 Å^3 (Al–GNS) and 361 Å^3 (Al–diamond), but the maximum porosity was less than 0.03%. The increase in pore volume in Figure 5 was accompanied by the increase in density in Figure 3, which further illustrates that graphene can facilitate a denser arrangement of Al atoms since pores with larger volumes can be formed in Al–graphene composites. Unexpectedly, the pore volume only decreased a bit at the diamond particles (R = 4.0 Å). That is, only a suitable ratio of 3D reinforcement to metal matrix can diminish the pores arising from the empty spaces between particles. Thus, it can be supposed that graphene may be beneficial for the formation of nanopores.

As a whole, the effects of graphene could be enlarged if evaluated as a function of the weight fraction. The curves of Al–graphene in Figures 3b and 5b increased faster than those in Figures 3a and 5a. This was mainly because the 2D material had an evident advantage related to its specific surface area. In conclusion, GNSs were deemed to have a greater impact on the inner structure of the metal matrix composite, and their high specific surface area could only explain a part of their impact.

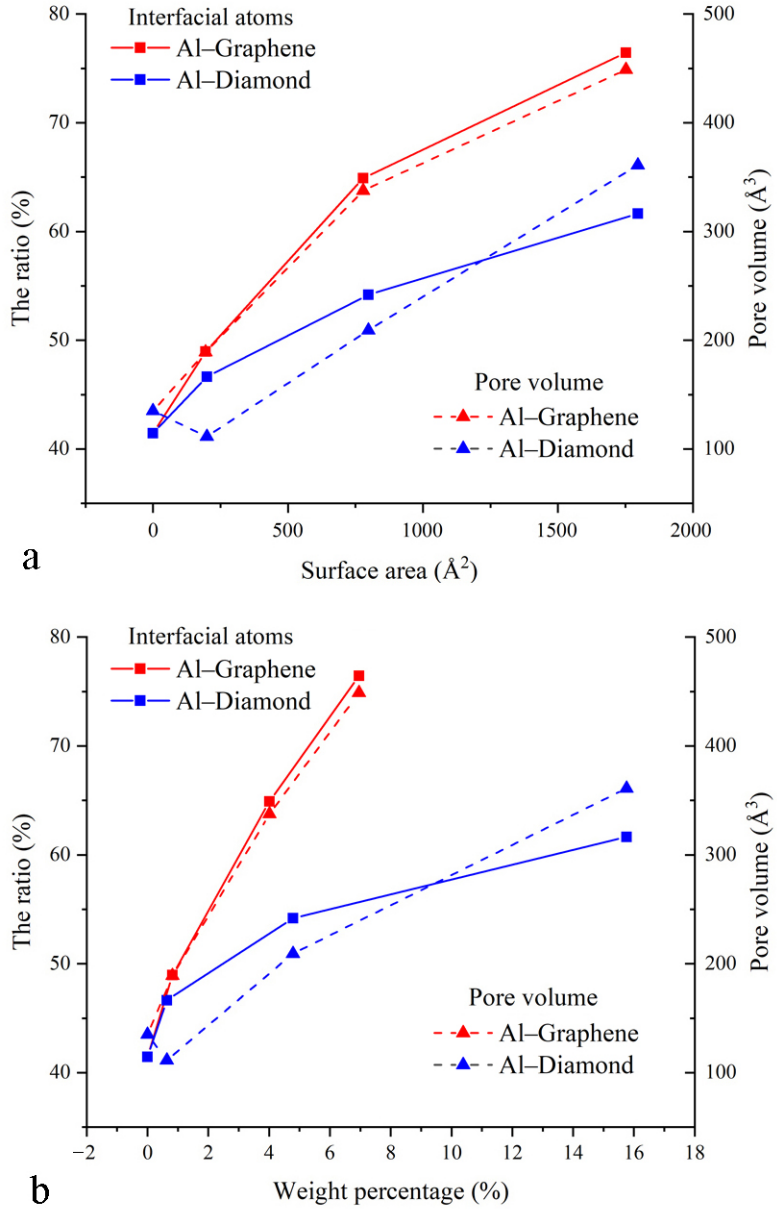

Figure 5. The ratios of Al atoms at grain boundaries and the pore volumes of the composites as functions of the surface area (**a**) and weight fraction (**b**).

3.3. The Tensile Process

In some MD studies based on simple models, the Al–graphene system is considered to have higher strength and greater ductility. However, that view is not supported by the models here. In this simulation, the tensile processes of every sintered system were conducted in three orthogonal directions. Then, the strength was calculated based on the average of the three tensile results. Because of the random directions of the GNSs, the tensile results in Table 2 do not distinctly display anisotropy in the Al–graphene composite. As shown in Figure 6, the strength of Al–graphene rose at first from 6.79 GPa to 6.87 GPa and then decreased to 6.51 GPa. The effects of the lateral sizes of GNSs on the mechanical properties of MMCs have been studied in experiments as well [21,22]. Because the ranges of the graphene contents in the experiments have been quite different, the influence of GNS size has differed. Ref. [21] revealed that the mechanical properties decreased with an increase in the lateral size of graphene, while Ref. [22] found that a composite with a moderate size exhibited the highest strength, and the results in Ref. [22] are consistent with

our models. Meanwhile, the strength of Al–diamond presented an early decrease from 6.95 GPa to 6.64 GPa and a later increasing trend up to 6.86 GPa. Distinctly, the composite with diamond (R = 4.0 Å) resulted in the highest strength, which may have corresponded to the lowest pore volume. When the sizes of the reinforcements reached their highest levels, a sharp reduction appeared for Al–graphene, but a clear increase emerged for Al–diamond after hitting the lowest level. This can be ascribed to the nano size of the Al grains, where the flow of the grain boundaries determined the strength of the MMC in accordance with the inverse Hall–Petch relation [23]. The effect of graphene was only greater than that of diamond at the weight fraction of 4%. Since the range of the variation in composite strength was no more than 5% and the curves were very complicated, the different reinforcements seemed to have no impact on the direct effects of tensile strength as well as ductility. An obvious reduction in ductility appeared in the composite with the biggest GNSs, which was also found in experimental studies [11–13]. The tensile processes of Al–graphene (l_s = 7.0 Å) and Al–diamond (R = 8.0 Å) were used as examples. The two curves in Figure 7 are nearly the same. During the evolution of inner structures at different strains, dislocations accumulated around the reinforcements, restricting the deformation of grains. Then, a crack extend between reinforcements. GNSs pulled from the matrix could not be found, which appeared in the simple models [4–6], leading to a big leap in tensile strength. This means that the direct effect of the reinforcements does not seem to have a heavy influence on the mechanical properties, which coincides with an investigation of a TiC particle-reinforced Al composite with a homogeneous distribution of dislocations [24]. Thus, the better result of the MMC strengthened by graphene should be mainly attributed to the greater effect of 2D materials on grain refinement.

Table 2. The tensile strengths of composites stretched in different directions.

Sizes of Reinforcements (Å)	Tensile Strength (GPa)			
	Along X Axis	Along Y Axis	Along Z Axis	on Average
\	6.80	6.83	6.71	6.78
l_s = 3.5	6.78	7.02	7.05	6.95
l_s = 7.0	6.53	6.70	6.69	6.64
l_s = 10.5	6.97	6.73	6.86	6.86
R = 4.0	6.79	6.88	6.72	6.79
R = 8.0	6.83	6.84	6.92	6.87
R = 12.0	6.62	6.26	6.63	6.51

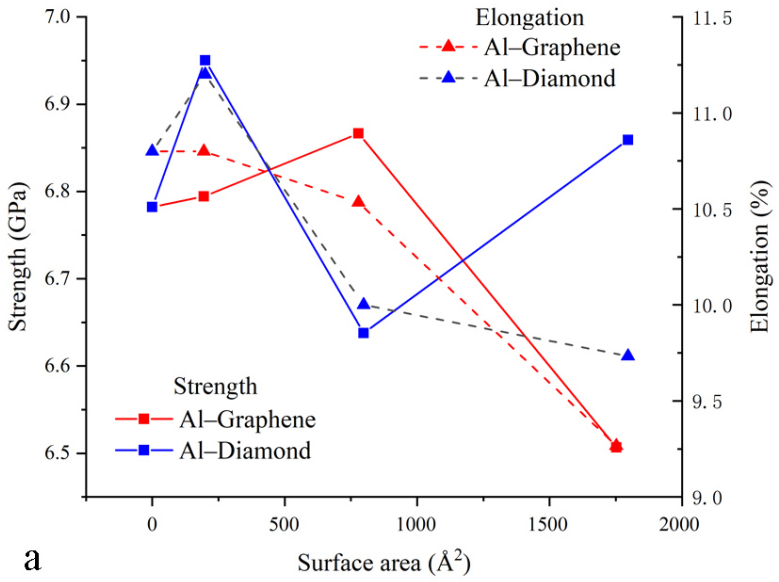

Figure 6. *Cont.*

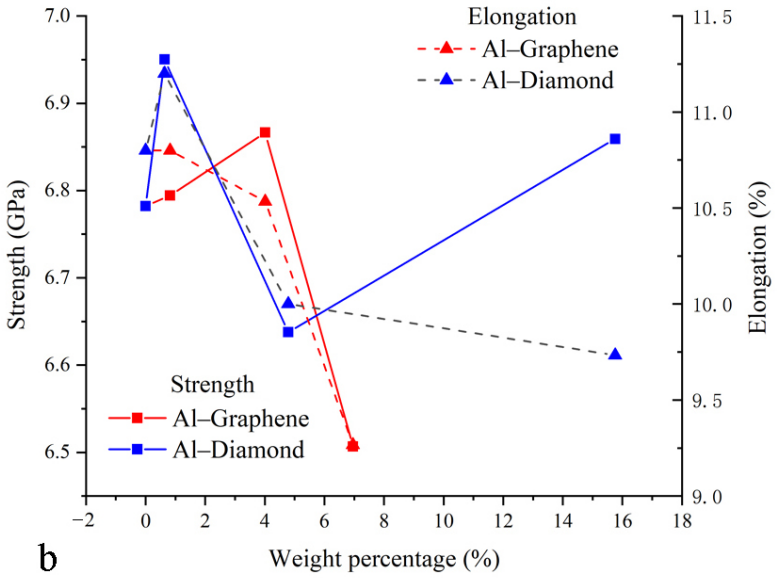

Figure 6. The tensile strength and elongation values of the composites as functions of the surface area (**a**) and weight fraction (**b**).

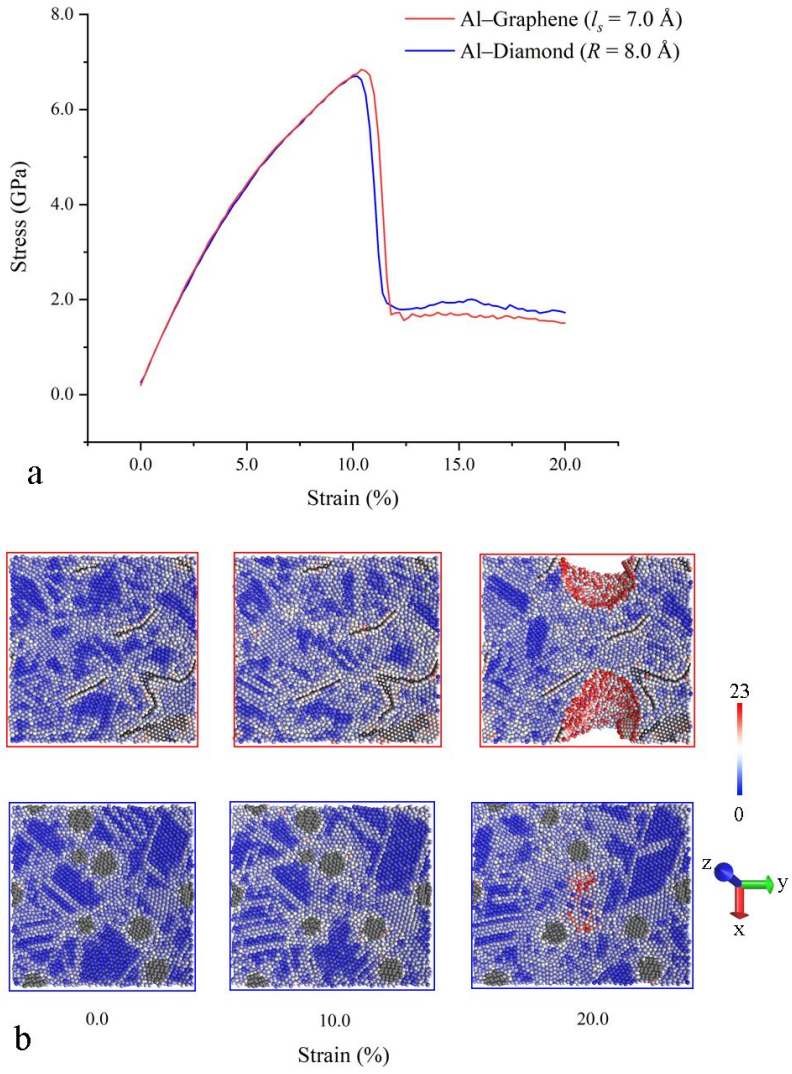

Figure 7. The stress–strain curves of the composites stretched in the Y direction (**a**) and the evolution of the inner structures at different strains (**b**).

4. Conclusions

Models with a larger scale were built to study Al matrix composites where GNSs or diamond particles were dispersed in random directions. A sintering process was carried out to achieve MMCs. Structural data and tensile results with respect to the surface areas of the reinforcements were obtained to compare the effects of the different reinforcements. With increases in the sizes of the reinforcements, the density of the Al–graphene composite could be 0.03 g/cc higher than the density of the Al–diamond, although it needed more heating time to complete densification. The GNSs were prone to form more pores, leading to an increase in pore volume from 135 $Å^3$ to 449 $Å^3$. A suitable ratio of 3D reinforcement to metal matrix may result in the fewest pores. The GNSs were also more conducive to grain refinement, as the ratio of Al atoms at grain boundaries grew from 41.4% to 76.4%. Because of the superiority of 2D materials when it comes to specific surface area, the effects of the GNSs on the composite structure could be enlarged at the same weight fraction of reinforcements. Thus, a denser MMC structure with finer grains could be prepared by introducing 2D reinforcements rather than 3D reinforcements with larger sizes. However, 2D materials seem to have no impact on the direct strengthening effect and did not result in anisotropy in the composite as reported in simple models. At the scale of these models, a reduction of 0.36 GPa in the tensile strength of the Al–graphene composite appeared when the GNSs grew to their largest size, and no enhancement of ductility was observed. During the evolution of the inner structures, the GNSs played the same role as the diamond particles, promoting the accumulation of dislocations. A crack originated at a position between the reinforcements, then went around the reinforcements. The greater improvements in the mechanical properties of the MMCs should be mainly ascribed to the advantage of the GNSs related to grain refinement. As far as the models described here are concerned, a composite with a moderate size exhibited the best mechanical properties. This result is supported by an experimental report.

Author Contributions: Conceptualization, Y.Z. and S.L.; methodology, Y.Z.; software, L.S.; validation, L.S., N.L. and C.S.; formal analysis, C.S.; investigation, N.L.; resources, N.L.; data curation, S.L.; writing—original draft preparation, Y.Z., L.S. and N.L.; writing—review and editing, S.L. and C.S.; visualization, Y.Z. and N.L.; supervision, S.L.; project administration, Y.Z.; funding acquisition, Y.Z. and S.L. All authors have read and agreed to the published version of the manuscript.

Funding: This research was supported by the Natural Science Foundation of Henan (242300420059 and 232300421344) and the key scientific research projects of colleges and universities in Henan Province (242102240022).

Data Availability Statement: The data presented in this study are available on request from the corresponding author due to [privacy].

Conflicts of Interest: The authors declare no conflicts of interest.

References

1. Tiwari, S.K.; Sahoo, S.; Wang, N.N.; Huczko, A. Graphene research and their outputs: Status and prospect. *J. Sci. Adv. Mater. Devices* **2020**, *5*, 10–29. [CrossRef]
2. Kumar, S.N.; Keshavamurthy, R.; Haseebuddin, M.R.; Koppad, P.G. Mechanical Properties of Aluminium-Graphene Composite Synthesized by Powder Metallurgy and Hot Extrusion. *Trans. Indian Inst. Met.* **2017**, *70*, 605–613. [CrossRef]
3. Kim, Y.; Lee, J.; Yeom, M.S.; Shin, J.W.; Kim, H.; Cui, Y.; Kysar, J.W.; Hone, J.; Jung, Y.; Jeon, S.; et al. Strengthening effect of single-atomic-layer graphene in metal-graphene nanolayered composites. *Nat. Commun.* **2013**, *4*, 2114. [CrossRef] [PubMed]
4. Zhao, S.; Zhang, Y.; Yang, J.; Kitipornchai, S. Folded graphene reinforced nanocomposites with superior strength and toughness: A molecular dynamics study. *J. Mater. Sci. Technol.* **2022**, *120*, 196–204. [CrossRef]
5. Liu, J.; Zhang, Y.; Zhang, H.; Yang, J. Mechanical properties of graphene-reinforced aluminium composite with modified substrate surface: A molecular dynamics study. *Nanotechnology* **2021**, *32*, 085712. [CrossRef]
6. Zhu, J.; Liu, X.; Wang, Z.; Yang, Q. Wrinkles-assisted nanocrystalline formation and mechanical properties of wrinkled graphene/aluminum matrix composites. *Model. Simul. Mater. Sci. Eng.* **2021**, *29*, 055017. [CrossRef]
7. Srivastava, A.K.; Pathak, V.K.; Singh, R.; Dikshit, M.K. Stress-strain behaviour of graphene reinforced aluminum nanocomposite under compressive loading using molecular dynamics. *Mater. Today Proc.* **2021**, *44*, 4521–4525. [CrossRef]

8. Elkady, O.A.; Yehia, H.M.; Ibrahim, A.A.; Elhabak, A.M.; Elsayed, E.M.; Mahdy, A.A. Direct Observation of Induced Graphene and SiC Strengthening in Al–Ni Alloy via the Hot Pressing Technique. *Crystals* **2021**, *11*, 1142. [CrossRef]
9. Lou, S.; Ran, L.; Liu, Y.; Chen, P.; Su, C.; Wang, Q. Effect of Hot Extrusion Ratio on the Mechanical Properties and Microstructure of a 0.5 wt.% Graphene Nanoplatelet-Reinforced Aluminum Matrix Composite. *J. Mater. Eng. Perform.* **2022**, *31*, 6533–6544. [CrossRef]
10. Zeng, M.; Chen, H.; Tao, X.; Ouyang, Y. Mechanical Property and Corrosion Behavior of Powder-Metallurgy-Processed 3D Graphene-Networks-Reinforced Al Matrix Composites. *Crystals* **2023**, *13*, 485. [CrossRef]
11. Zhou, S.; Zhang, W.; Liu, M.; Ren, W.; Yang, Y.; Zhou, Q.; Ma, S.; Shi, L. Microstructure evolution and tensile properties tailoring of graphene nanoplatelets/nickel composites fabricated by two-step 3D vibration milling. *J. Alloys Compd.* **2022**, *918*, 165676. [CrossRef]
12. Yang, W.; Zhao, Q.; Xin, L.; Qiao, J.; Zou, J.; Shao, P.; Yu, Z.; Zhang, Q.; Wu, G. Microstructure and mechanical properties of graphene nanoplates reinforced pure Al matrix composites prepared by pressure infiltration method. *J. Alloys Compd.* **2018**, *732*, 748–758. [CrossRef]
13. Wang, J.; Guo, L.-N.; Lin, W.-M.; Chen, J.; Liu, C.-L.; Zhang, S.; Zhen, T.-T. Effect of the graphene content on the microstructures and properties of graphene/aluminum composites. *New Carbon. Mater.* **2019**, *34*, 275–285. [CrossRef]
14. Wang, Z.-G.; Li, C.-P.; Wang, H.-Y.; Zhu, X.; Wu, M.; Jiang, Q.-C. Effect of nano-SiC content on mechanical properties of SiC/2014Al composites fabricated by powder metallurgy combined with hot extrusion. *Powder Metall.* **2016**, *59*, 236–241. [CrossRef]
15. Kumar, G.B.V.; Panigrahy, P.P.; Nithika, S.; Pramod, R.; Rao, C.S.P. Assessment of mechanical and tribological characteristics of Silicon Nitride reinforced aluminum metal matrix composites. *Compos. Part B Eng.* **2019**, *175*, 107138. [CrossRef]
16. Sharma, P.; Sharma, S.; Khanduja, D. Production and some properties of Si_3N_4 reinforced aluminium alloy composites. *J. Asian Ceram. Soc.* **2015**, *3*, 352–359. [CrossRef]
17. Zhu, Y.; Li, N.; Li, W.; Niu, L.; Li, Z. Atomistic Study on the Sintering Process and the Strengthening Mechanism of Al-Graphene System. *Materials* **2022**, *15*, 2644. [CrossRef]
18. Sun, H.; Li, N.; Zhu, Y.; Liu, K. A Model for Direct Effect of Graphene on Mechanical Property of Al Matrix Composite. *Metals* **2023**, *13*, 1351. [CrossRef]
19. Dandekar, C.R.; Shin, Y.C. Molecular dynamics based cohesive zone law for describing Al–SiC interface mechanics. *Compos. Part A* **2011**, *42*, 355–363. [CrossRef]
20. Han, R.Q.; Song, H.Y.; An, M.R. Atomic simulation of interaction mechanism between dislocation and graphene in graphene/aluminum composites. *Comput. Mater. Sci.* **2021**, *197*, 110604. [CrossRef]
21. Porwal, H.; Saggar, R.; Tatarko, P.; Grasso, S.; Saunders, T.; Dlouhý, I.; Reece, M.J. Effect of lateral size of graphene nano-sheets on the mechanical properties and machinability of alumina nano-composites. *Ceram. Int.* **2016**, *42*, 7533–7542. [CrossRef]
22. Zhao, M.; Xiong, D.-B.; Tan, Z.; Fan, G.; Guo, Q.; Guo, C.; Li, Z.; Zhang, D. Lateral size effect of graphene on mechanical properties of aluminum matrix nanolaminated composites. *Scr. Mater.* **2017**, *139*, 44–48. [CrossRef]
23. Conrad, H.; Narayan, J. On the grain size softening in nanocrystalline materials. *Scr. Mater.* **2000**, *42*, 1025–1030. [CrossRef]
24. Krajewski, P.E.; Allison, J.E.; Jones, J.W. The influence of matrix microstructure and particle reinforcement on the creep behavior of 2219 aluminum. *Metall. Mater. Trans. A* **1993**, *24*, 2731–2741. [CrossRef]